Indonesian Journal of Pharmacy

VOL 35 (2) 2024: 194–210 | REVIEW ARTICLE

Advances in Quantitative and Qualitative Assessment of Collagen in Cutaneous Wound Healing

Clarissa Nadya Santoso, K. Ariex Widyantara, Nyoman Bayu Wisnu Kencana, F.D. Erika Setyajati, Agustina Setiawati*

Faculty of Pharmacy, Sanata Dharma University, Paingan, Maguwoharjo, Depok, Sleman, Yogyakarta, Indonesia 55281.

Article Info

Submitted: 05-09-2023
Revised: 19-01-2024
Accepted: 19-02-2024

*Corresponding author
Agustina Setiawati

Email:
nina@usd.ac.id

ABSTRACT

Wound healing treatment is a challenging strategy in skin drug delivery due to its complexities. During wound healing stages, fibroblasts deposit extracellular matrix components, which majority is collagen. Issues related to collagen production, including scar formation, and delayed wound healing are essential in wound healing research. Hence, recent studies have focused on assessing macroscopic and microscopic collagen fibers qualitatively and quantitatively. Macroscopic analysis of collagen includes two-dimensional (2D) photographs, planimetric assessments, ultrasonic imaging, and 3D scanning of wounds; as well as histology-based microscopically scoring. Thus, the quantitative assessment of collagen involves Scar Index quantification and collagen content measurement using ImageJ. To date, a comprehensive analysis combining those methods could provide insight for pharmacists, dermatologists, and skin researchers to conduct a precise assessment of the wound healing process.

Keywords: skin, scar, extracellular matrix, dermatologist

INTRODUCTION

The human skin makes up 15% of the body weight, making it the largest tissue in the body. It serves mainly as a barrier of protecting, and preventing internal structures from drying out and cracking mechanically, chemically, thermally, or from light. Human skin, with its vital protective functions, is perpetually exposed to physical damage, heightening the risk of harm (Takeo *et al*., 2015). In response, Caetano *et al*. (2016) assert that the skin has evolved a dynamic wound-healing process to ensure survival, involving the remodeling of damaged tissue architecture. The wound environment is abundant in the extracellular matrix (ECM), as ECM intricately governs the complex regulation of wound healing (Rodrigues *et al*., 2019).

The wound-healing process is a complex sequence of events, loosely divided into 4 coinciding stages: hemostasis, inflammation, proliferation, and remodeling (Murphy & Evans, 2012). It begins immediately after tissue injury. Growth factors, platelet granules, and cytokine molecules are released to regulate inflammatory cells during wound healing. This cellular invasion is essential for local debridement during the inflammatory phase. These cells help get rid of unwanted items and act as a matrix for fibroblasts to grow into larger cells, which forms granulation tissue finally (Gurtner *et al*., 2008; Velnar *et al*., 2009).

When tissue is injured, fibroblasts rapidly multiply and move to the damaged area. There, they initiate a fresh extracellular matrix (ECM) by producing components like proteoglycans, glycosaminoglycans, and collagen. This new ECM replaces the temporary one that forms initially after injury (Velnar *et al*., 2009; Guo & DiPietro, 2010). Collagen, a predominant protein in the human body, serves as a critical building block for the extracellular matrix (ECM) of human skin. It plays a vital role in every phase of wound healing, acting as a chemical guide to facilitate the process (Pfisterer *et al*., 2021; Dong *et al*., 2021). Additionally, research by Yang & Kang (2019) further emphasizes that collagen facilitates tissue repair by enhancing cell adhesion, chemotaxis, and migration. There are 29 types of collagen; but the key role in the wound healing process is collagen type I and II (Owczarzy *et al*., 2020). A study by Ho & Hantash (2013) found that the significance of analyzing collagen in wound healing arises from

the effects of deficient collagen production during the healing process. Researchers have developed various assays to assess wound healing, examining collagen presence both qualitatively and quantitatively through macroscopic and microscopic methods (Rezakhaniha *et al*., 2012; Quan & Fisher, 2015; Theunissen *et al*., 2016; Matsumoto *et al*., 2021; Jørgensen *et al*., 2020; Bien *et al*., 2014). The macroscopic assessment of wounds relies on two types of examinations: visual observation and spatial measurements. This measurement includes two-dimensional (2D) photographs of wounds, planimetric assessments of wounds, and three-dimensional scanning of wounds (Jørgensen *et al*.,2020, Bien *et al*., 2014; Jin, 2018). All those methods must be combined with a microscopical assessment of collagen in the dermis (Zhou *et al*., 2019). Dermal histology after haematoxylin eosin shows that normal collagen fibers are thick and irregularly arranged, whereas scar collagen fibers are thin and flattened (Limandjaja *et al*., 2017). The increase in collagen synthesis and excessive collagen is a result of scarring conditions including keloids and hypertrophy (Ho & Huntash, 2013). Traditionally, collagen fibers have been visually graded by trained raters from rank 0 to 4+, resulting in less accuracy and high subjectivity (Chlipala *et al*., 2020). However, these methods could be biased and have high subjectivity due to the grade variability of staining reagent, high subjectivity between evaluators, and result inconsistency in a study (Brianezi *et al*., 2015, Schipke *et al*., 2017; Gole *et al*., 2020). Thus, measuring the structural and ultrastructural collagen of healing wounds continues to pose challenges.

As the exploration of innovative therapeutic healing agents gains greater importance, there remains a constant demand for dynamic assessments of wound healing (Mirhaj *et al.*, 2022; Freedman *et al*., 2023; Kolimi *et al.*, 2022). Recent strides in computer technology, exemplified by advanced programs like Image J, have revolutionized studies to perform dynamic functional imaging by seamlessly linking multiple data sources to establish comprehensive quantitative systems. This review offers an extensive examination of collagen assessment within the wound healing process, encompassing both macroscopic and microscopic evaluations. We delve further into the discussion of quantitative and qualitative assessment of collagen fibers at the microscopic level within this review.

SKIN WOUND HEALING

Human skin primarily acts as a defensive barrier, protecting internal structures from dehydration and harm caused by physical, chemical, thermal, and light factors (Takeo *et al*., 2015). As a defensive barrier, the skin has to strengthen its response to pathogens. (Naik *et al*., 2015). Consequently, skin tissue has to advance its process in wound healing.

Cellular Responses Underlying Wound Repair

The process of wound healing is complex and dynamic, involving interactions among various cells and molecules (Enoch & Leaper, 2008) It encompasses four stages, the first is hemostasis, followed by inflammation, proliferation, and the last is remodeling (Singer & Clarck, 1999).

Haemostasis

The wound healing process starts with the hemostasis phase, which is characterized by immediate constriction, disruption, and blood vessel extravasation. Normal hemostasis steps depend on interactions between vascular platelets and clotting factors. Hemostasis stages are intended to prevent massive blood loss upon injury by regulating blood flow under normal physiological conditions (Zaidi & Green, 2019). Tiny anucleate cells floating in our blood, called platelets, play a crucial role in stopping bleeding and forming clots. When a tissue is damaged, collagen accumulates at this site and activates platelets to produce a hemostasis plug. Meanwhile, a protein called Tissue Factor (TF) begins the production of clotting factor activators and thrombin to provide the production of thrombin (Clark, 2003). Thrombin converts a protein called fibrinogen into fibrin, creating a mesh-like structure. This mesh acts as a provisional extracellular matrix, providing a platform for cells to migrate and start the healing process. Platelet-containing clots essentially serve to seal wounds and provide a substrate for inflammatory cell formation (Zaidi & Green, 2019). A high density of platelets that store vasoactive amine molecules such as serotonin to increase microvascular permeability. Platelets express many Toll-like receptors (TLRs) (Cognase *et al*., 2005). It regulates the production of antimicrobial peptides. In addition, immune cells activate platelets in the wound site either by directly trapping them or by releasing chemokines (Tang *et al*., 2002; Golebiewska & Poole, 2015). Rodrigues *et al*. (2019) found that,

in haemostasis, platelets are essential, and their absence disturbs the wound healing process.

Inflammation

The inflammatory stage comprises both early and late phases (Enoch & Leaper, 2008). Within 24–48 hours after injury, chemoattractants like ECM, transforming growth factor-β (TGF-β), and formyl-methionyl peptides attract neutrophils to the wound site. These neutrophils transform into activated macrophages, releasing growth factors named endothelial and vascular endothelial growth factors. A study by Enoch & Leaper (2008) found that neutrophils cohere with endothelial cells and migrate within blood vessels. Neutrophils swamp pathogens by generating oxygen-derived degradative enzymes and free radicals. Meanwhile, cells at the wound site in the skin epidermis gain mitotic activity to migrate and proliferate along the dermis.

During the final stage of inflammation, collagen forms at the wound incision margins (Enoch & Leaper, 2008). Inflammation in wound healing is a complex process regulated by various intrinsic and extrinsic factors. The following are examples of external factors: temperature, humidity, chemicals, desiccation, mechanical stress, debris, and medication status (Dhasmana *et al*., 2021). Reduced levels of monocytes and macrophages disrupt the wound-healing process. This leads to inadequate removal of damaged tissue (debridement), delayed fibroblast cell growth, impaired growth of fibrosis, and the formation of new blood vessels. In cases of uncontrolled inflammation, such as observed in diabetic mice, healing is significantly delayed (Boniakowski *et al*., 2017).

Proliferation

The proliferative phase involves fibroblast relocation, extracellular matrix deposition, and the formation of granulation tissue. This phase begins three days after injury and continues for two to four weeks. During proliferation, fibroblasts play a crucial role in replacing the temporary fibrin matrix within the freshly synthesized granulation tissue (Wilkinsoon & Hardman, 2020). These fibroblasts also express matrix metalloproteinases (MMPs), which break down the temporary matrix and substitute it with granulation tissue that is rich in fibronectin, proteoglycans, and collagen in its immature stage (Enoch & Leaper, 2008). Once a sufficient collagen matrix is deposited, fibroblasts cease collagen production and undergo apoptosis triggered by unknown signals. It functions as a structure supporting the production of new vascular deposits in the ECM, wound cell migration, and differentiation (Wilkinson & Hardman, 2020). Granulation tissue indicates a wound healing process when it is moist, shiny, and has a reddish appearance. On the other hand, an overly soft, brittle, and dark red color indicates inadequate healing (Enoch & Leaper, 2008).

Neovascularization supplies the metabolic demands of rapidly growing healing tissue called angiogenesis. This stage is driven by hypoxia, which activates hypoxia-inducible factor (HIF), cyclooxygenase-2 (COX-2), and subsequent VEGF release (Huang *et al*., 2005). Additionally, several molecules reveal angiogenic activity, involving TGF-β, angiotropin, angiogenin, angiopoietin 1, and thrombospondin (Golebiewska & Poole, 2015). Angiogenesis is triggered by these molecules because this molecule induces endothelial and basic fibroblast growth factors through macrophages and endothelial cells.

Re-epithelialization

The epidermis, which forms the surface layer of human skin, consists of a stratified epithelial tissue primarily composed of keratinocytes. However, beyond keratinocytes, the epidermal layer also accommodates immune cells, hair follicles, sebaceous glands, and sweat glands. When the skin sustains an injury, dermal fibroblasts communicate via the Wnt/β-catenin pathway with hair follicle stem cells. These stem cells relocated to the wound site, differentiate, and replace various types of epidermal cells. Conversely, stem cells stimulate fibroblasts thus they transform into myofibroblasts, which play a role in wound contraction (Rodrigues *et al*., 2019). Additionally, stem cells multiply, forming non-conjugating keratinocytes that relocate to the damaged site and contribute to re-epithelialization. Caetano *et al*. (2016) state that This process is facilitated by the discharge of growth factors and the activation of receptors responsive to growth factors.

Remodeling and Tissue Maturation

When the re-epithelialization process finishes, myofibroblasts within the granulation tissue engage in continuous production of matrix metalloproteinases and their specific inhibitors. These MMPs, which are produced by various cell types including macrophages, epidermis cells, fibroblasts, and endothelial cells, play a crucial role

in producing the tissue (Caley *et al*., 2015; Chen, 1992). During this remodeling stage, specific components of the extracellular matrix (ECM) are broken down by MMPs. Notably, the regulation of MMP activity is delicate because essential collagen must be preserved to avoid hindering the wound-healing process. As the healing process progresses, collagen synthesis and degradation reach a steady state approximately 21 days after the injury. Macrophages contribute significantly to wound healing by clearing away ECM debris and apoptotic cells. This continuous skin reconstruction eventually leads to a metalloproteinase activity impeding and tissue inhibitor metalloproteinase decreasing. Furthermore, the density of macrophages and fibroblasts decreases. While the tissue matures, fibronectin and hyaluronan are broken down, and the diameter of collagen fibers increases

THE ROLES OF COLLAGEN FIBER AND ITS ABNORMALITIES IN WOUND HEALING

Dermal collagen, constituting around 80% of the dermis's dry weight, is the primary protein responsible for organizing the extracellular matrix (ECM), including skin (Babalola *et al*., 2014). Fibroblasts in the skin dermis play a vital role in creating, arranging, and maintaining the collagen-rich connective tissue (Quan & Fisher, 2015). The papillary dermis and the reticular dermis are two types of skin dermis (McGrath, 2020). While the papillary dermis contains only small amounts of collagen, the reticular dermis houses more abundant collagen bundles. There are 29 different forms of collagens found in vertebrate tissues, which can be divided into two main groups: non-fibrillar collagens (types IV, VI, VIII, XIV, and XVII) and fibrillar collagens (types I, III, and V) (Wang, 2021). About 80% of the collagen in the human body is type I collagen, which also predominates in the dermis. Non-fibrillar collagen is less important than fibrillar collagen (Wang, 2021). Due to its widespread presence, collagen I is believed to exist in nearly all connective tissues (McGrath, 2020).

Fibroblasts, obtained from the dermis at wound edges, have a vital role in collagen synthesis, which forms the primary item of mature connective tissue scars (Brook, 1995). The strength of healed skin depends on the type, quantity, and structure of collagen, which changes during the healing process. Initially, COL III is produced, followed by replacement with collagen I, the dominant collagen type in the skin (Mathew-Steiner *et al*., 2021; Rangaraj *et al*., 2011). At the wound site, collagen IV and VII (COL-IV and VII) are evenly distributed, with no time-dependent variation in their appearance in injured skin, such as in surgical wound sites (Velez & Howards, 2012). COL-IV is found in the reticular dermis, subcutaneous tissue, and papillary dermis. According to immunofluorescent detection in cryosections of human neonatal foreskin tissue, papillary dermal expression of COL-IV is higher. COL-IV is present in the dermis of adult skin samples, especially in the vicinity of the vasculature and papillary dermis. Prior research indicates that COL-IV is not produced within the wound itself, but rather more intensely around the wound borders on days 1 through 3. Nevertheless, the re-epithelialization incision's granulation tissue rises after 7 days (Theocharis *et al*., 2016).

When activated, myofibroblasts assume the critical role of synthesizing and depositing components of the extracellular matrix (ECM) (Huang *et al*., 2020). These specialized cells also contribute significantly to granulation tissue contraction and maturation1. Growth factor-β1 (TGF-β1) is responsible for converting fibroblasts into myofibroblasts, leading to an increase in collagen production (Petrov *et al*., 2002). Smooth muscle α-actin (SMA) expression and other pro-fibrogenic characteristics, such as TGFβ1, type I/III collagen, and tissue inhibitor of metalloproteinase-1 (TIMP-1), which functions as a collagenase inhibitor, determine the myofibroblast phenotype. (Duong & Hagood, 2018). During the early stages of granulation tissue formation, myofibroblasts primarily produce collagen III, influencing the size of collagen I fibers. Initially, collagen III expression outpaces collagen I, resulting in a higher ratio of the two collagen subtypes (from 20% to 50%) (Xue & Jackson, 2015). As the scar matures, this ratio normalizes, allowing the identification of immature scars by their elevated collagen III content compared to collagen I.

In addition to their ability to produce more collagen and less collagenase than fibroblasts, scar myofibroblasts are less susceptible to apoptotic signaling, which may play an important role in scar formation. (Moulin *et al*., 2004). Cytokines such as basic fibroblast growth factor (bFGF), fibroblast growth factor-2 (FGF-2), interferon-gamma (IFN-γ), and interleukin-1 (IL-1) can suppress TGFβ1-mediated fibrogenesis (Duong & Hagood, 2018).

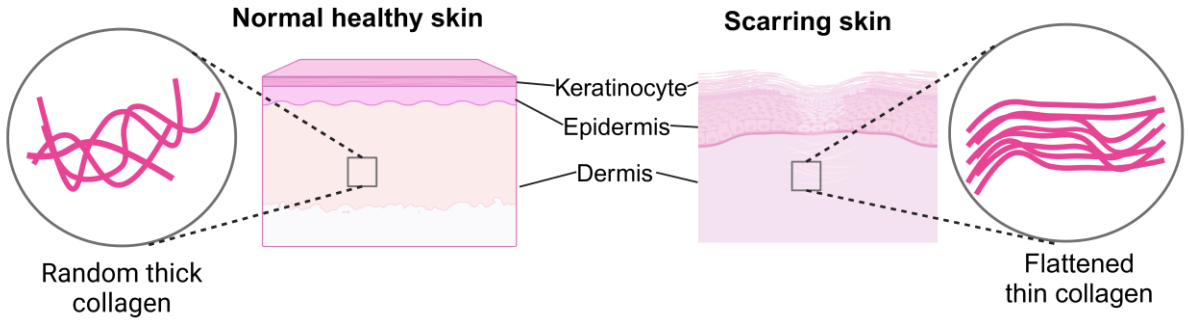

Figure 1. The collagen arrangement in scarring versus normal, healthy skin

Decreased collagen numbers induce myofibroblast apoptosis as a result of these cytokine activities (Potekaev *et al*., 2021). When the researchers compared scar fibroblasts with their normal counterparts, they found that collagenase mRNA was reduced and their ability to digest soluble collagen was also reduced (Zhu *et al*., 2013). Inappropriate myofibroblast apoptosis leads to excessive scar formation (Huang *et al*., 2020).

Collagen fibers in normal human skin tissue are found in random basket weave structures. In human scars, collagen forms unidirectional crosslinks parallel to the skin (Figure 1) (Xue & Jackson, 2015). Compared to normal tissue, scar tissue has higher collagen density and larger fiber size (Wolfram *et al*., 2009). Thicker collagen fibers and parallel arrangement increase the tensile strength of the tissue. Most collagen fibrils in normal skin are composed of collagen I and collagen III. Instead of simple collagen fibers, the dermis consists of a highly ordered extracellular matrix (ECM) network, fused into a network composed primarily of collagen (McGibbon, 2005). Collagen fibrils play an important role in restoring tension during tissue healing, whose tension is greater than the total tension of autologous cells (Brauer *et al*., 2019).

Qualitative Analysis of Wound Healing
Macroscopically Wound Assessment
Two-dimensional photographs of wounds

Clinical methods have predominantly utilized two-dimensional (2D) approaches for measuring wounds Jørgensen *et al*. (2020). The assessment of wounds relies on two types of examinations: visual observation and spatial measurements. The visual evaluation involves analyzing attributes such as size, texture, color, tissue composition, and the stage of severity. The methods for spatial measurement encompass estimating wound area through conventional rulers, transparent tracing, injection of colored dyes, and the creation of molds using alginate (Dhane, 2016). Wound segmentation in two dimensions involves various techniques such as K-means clustering, deep neural networks, support vector machines, k-nearest neighbors, and basic feedforward networks. Additional methods encompass superpixel region-growing algorithms, color histograms, and the utilization of both geometric and visual characteristics of the wound surface to achieve wound segmentation (Filko, 2023). The most popular methods by far implement deep neural networks.

A specialized deep neural approach can identify the location of the wound, separate it from the distracting background, and locate its position. Thus, it generates a highly reproducible map of wound segmentation without user intervention and standardizes image acquirement during analysis (Scebba *et al*., 2022). Wang *et al*. (2020) introduced a deep convolutional neural network design named MobileNetV2 for wound segmentation. Before actual training, the network was strained using the Pascal VOC dataset. The resultant neural network model produced a segmented grayscale wound image as output, where each pixel carried a probability value denoting its likelihood of being a wound pixel. Subsequently, this image underwent a sequence of post-processing steps, including thresholding to establish an initial binary image, hole filling, and the elimination of minor regions. These steps culminated in the generation of a definitive binary image or segmentation mask. Mahbod *et al*. (2021) introduced a segmentation method that combines the U-Net and LinkNet deep neural networks. These networks fundamentally consist of encoder-decoder convolutional architectures.

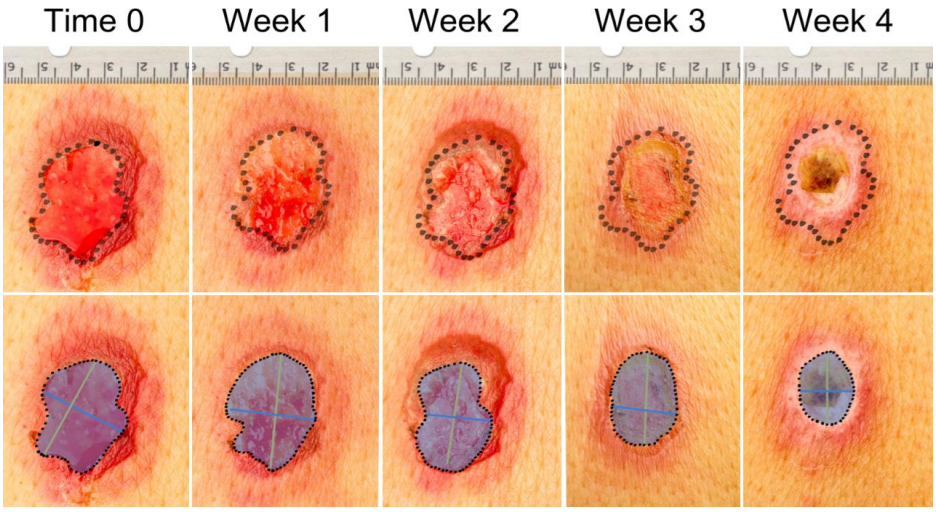

Figure 2. Measuring the dimension of the lesion using Digital Planimetry and Ruler Technique (adapted from Bien *et al*., 2014)

Planimetric assessments of wounds

The technique for measuring wound area using planimetric software (or graphical software equipped with suitable functions) along with digital photographs is favored due to its simplicity and cost-effectiveness. In this approach, a photograph of the wound is taken with a ruler or known-size marker positioned alongside the wound's edge. The image is then transferred to a computer and opened in planimetric software (Figure 2). The ruler or marker serves as a reference for scaling the linear dimensions within the image. After manually tracing the wound border using a computer mouse, the software calculates and presents the wound's area (Foltynski, 2015). The surface area of a skin lesion can also be assessed by outlining the lesion's borders on transparent acetate placed over it and then calculating the number of square centimeters within the outlined area using a grid. While this method is relatively straight forward and offers good reliability, there can be variations in results when deciding whether to include partially covered squares within the outline. Digital planimetry might offer a more accurate and objective alternative to the grid-counting method for determining wound surface area, particularly for irregularly shaped wounds (Bien *et al*., 2014).

The computer-based planimetric evaluation of lesions was conducted manually. In the initial step, the physician loaded a digital photograph of a pressure ulcer into the program and subsequently outlined the contours of the lesions. Once the selection phase is complete, the software automatically computes the area enclosed by the predetermined outline. This area measurement is expressed in pixels or, following appropriate calculations, in square centimeters. To convert the area into square centimeters, it's essential to adjust the distance between the camera lens and the analyzed body part accurately. This calibration process involves marking the body part during the capturing process (Senejko, 2021).

3D Three-dimensional scanning of wounds

Various three-dimensional (3D) wound assessment devices have been developed. These encompass laser scanning tools, methods based on structured light, digital imaging techniques, and systems using stereophotogrammetry (SPG) technology. These 3D devices can assess wound healing from a volumetric perspective. The adoption of 3-D scanning technology for measuring wound dimensions in scenarios like burns and cuts has gained considerable interest. Some researchers have also explored its utility for appraising scars. Earlier investigations required the utilization of two to three cameras concurrently capturing images of the scar to generate 3-D data. However, they are not extensively employed in clinical settings due to several practical constraints, such as imprecision, high expenses, time-intensive procedures, and complexities in operation (Jin, 2018; Jørgensen, 2020).

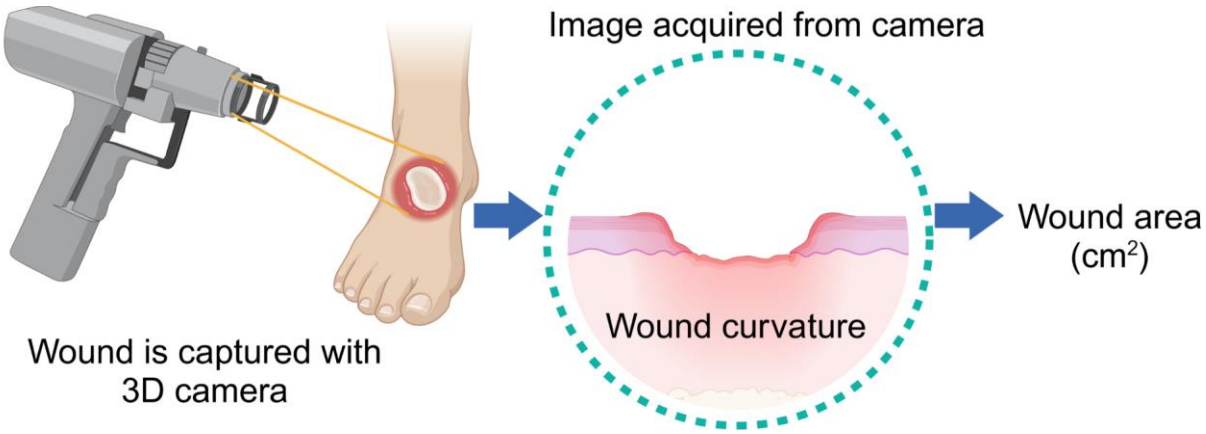

Figure 3. The 3D-WAM imaging of a diabetic foot ulcer (adapted from Jørgensen *et al.,* 2020). The image was prepared in Biorender.

Lasers are commonly utilized for 3D reconstruction. In this process, a laser line projection sensor, in conjunction with an RGB camera, is frequently used to generate detailed and colored 3D reconstructions. One of the initial instances where such an approach was employed was demonstrated in the Derma study, where the authors utilized the Minolta VI910 scanner. Similarly, the fusion of laser technology and RGB cameras was also evident in related research endeavors. While these systems have displayed a remarkable level of precision, they do come with the challenge of complex operation. Additionally, a constraint of these investigations was the necessity for the entire wound to be visible within a single frame (Filko, 2023).

Another method of 3D wound measurement was a 3D wound assessment monitor (WAM) camera, which can calculate wound area in three dimensions and is capable of assessing wound characteristics. The handheld device known as the 3D-WAM camera is a creation of the Danish company Teccluster. This 3D camera is constructed with a projector and a trio of cameras incorporated into a single unit. The measurement process for wounds was carried out in a standardized manner. Using this arrangement, the wound is photographed from various angles (one photo is taken parallel to the wound) while maintaining a consistent distance, guided by two red markers indicating the wound's location. Following this, the images are merged into a single 3D representation on a computer screen by identifying corresponding points in the photos. Next, the outline of the wound's edge is manually traced on the screen, and the software of the 3D-WAM camera promptly calculates the wound's size (Figure 3) (Jørgensen *et al*., 2020).

Ultrasound imaging of wounds

Ultrasound imaging offers rapid, cost-effective, radiation-free, non-intrusive, and point-of-care imaging capabilities, allowing for deep visualization into soft tissues up to a depth of about 10 cm (Mantri, 2021). Ultrasonography can non-invasively evaluate the structure, blood flow, and elasticity of tissues, which are essential aspects for assessing wound healing. Furthermore, ultrasound has been validated as a reliable method for gauging wound size, a critical factor in tracking how wounds heal over time. Moreover, tissue composition changes and scarring are also possible to be identified. It enables the measurement of biological tissue characteristics by analyzing acoustic properties like velocity, attenuation, absorption, and tissue scattering of echoes. Thus, ultrasonography has enabled detailed examination of the skin surface and the mapping of tissue elasticity (Gynwali, 2020).

A researcher gathered ultrasound images using a portable ultrasound system equipped with a 5–18-MHz probe, which offers satisfactory clarity for imaging 20–30 mm beneath the skin's surface. The ultrasound scans operated at an 18 MHz frequency. For infection prevention, a disposable plastic cover was placed over the probe before scanning. The ultrasound gain was fine-tuned to the best level for each instance. The focus point was positioned at the subcutaneous tissue depth based on the soft tissue thickness. During ultrasound

scanning, videos were recorded with the probe directed both transversely and longitudinally. The probe was shifted from the healthy region to the pressure injury area by navigating through the skin around the wound. Subsequently, we analyzed an image extracted from the ultrasound videos showing the wound and the skin surrounding the wound (Matsumoto *et al*., 2021).

Histology based Microscopically Scoring

Various methods have been developed to assess wound healing clinically, one of them was based on the histological state of the skin. Histological assessment should involve the fundamental aspects of wound healing such as inflammation, angiogenesis, fibroplasia, and connective tissue development.

One of the most common methods to analyze various tissue healing or pathology at the microscopic structural level is hematoxylin eosin staining (Nurrahma *et al*., 2022; Mutiah *et al*., 2020, Wardani *et al*., 2022; Pananchery & Gadgoli, 2021). Histopathological staining using hematoxylin-eosin (HE) is one of the most common analytical methods. This gold standard has been employed for assessing histology for over 100 years (Osman *et al*., 2014). After being standard stained with HE, the wound healing process can be evaluated by respectively observing the re-epithelialization of the epidermis layer through epithelial thickness HE stains of wounded skin (Wardani *et al*., 2022; Setiawati *et al*., 2021). Thus, the quality of wound healing is also determined by inflammatory cell penetration on the wounded area including neutrophils, basophils, and macrophages (Pananchery & Gadgoli, 2021). Therefore, a semi-quantitative scale was utilized, assigning scores ranging from 0 to 4 based on characteristics related to density, mitotic activity, and epithelial growth. The parameters are based on re-epithelialization, granulation, inflammatory cells, and angiogenesis. Re-epithelialization ranks 4 on the score of 80% epidermal remodeling. Granulation processes are scored 0 to 4, in which the 4 presents a complete 80% tissue organization. Thus, the inflammatory cells' existence at 0 scores refers to 13-15 inflammatory cells in each histological field. On the other hand, 4 score refers to 1-4 cells per inflammatory cell. Moreover, another important parameter of the healing process is angiogenesis, which is evaluated by counting vessels at each histological site. The presence of 7 vessels per vertical site of epithelial cells is given a maximum score of 4, while the absence of blood vessels and the presence of hemorrhaged edema were evaluated score of 0 (Theunissen *et al*., 2016).

The epidermis was evaluated using a simplified 3-point scale, which depended on the extent of rete ridge restoration. The assessment of the papillary and reticular dermis involved comparing them to normal skin, considering factors such as collagen fiber alignment, density, and maturity. It's worth noting that this scale, known as the Histologic Assessment Scale, has been previously validated and proven to be a dependable and consistent tool for evaluating human wounds histologically (Theunissen *et al*., 2016).

The utilization of computerized wound image analysis represents an objective, reproducible, and precise approach for interpreting both qualitative and quantitative macro-morphological changes that occur in a wound throughout the healing process. This method involves converting computerized data into images, facilitating the analysis, quantification, and presentation of wound characteristics, thereby significantly enhancing the reproducibility of wound image assessments and their resulting data. This approach offers a more comprehensive evaluation compared to basic morphometric measurements and is less reliant on subjective judgment than traditional histopathologic scoring systems. This review explains particularly computerized methods for collagen orientation analysis.

Analysis of collagen microstructure is of critical importance in the study of wound healing, as collagen alignment is one of the wound healing assessments of skin tissue. Under a light microscope, scientists focus on the dermis layer, where granulation tissue resides. The critical factor to evaluate is collagen fiber orientation. In normal dermal tissue, collagen fibers exhibit a loose and random arrangement, akin to a basket weave. However, in cases of dermal scarring, the collagen orientation appears flat within the dermis layer (Figure 1) (Limandjaja *et al*., 2017; Zhou *et al*., 2019). Traditional methods for assessing collagen density rely on subjective visual rankings by trained raters, ranging from 0 to 4+ (Chlipala *et al*., 2020; Brianezi *et al*., 2020). Additionally, specific immunohistochemical staining for COL-1 protein provides valuable insights for evaluating the wound healing process.

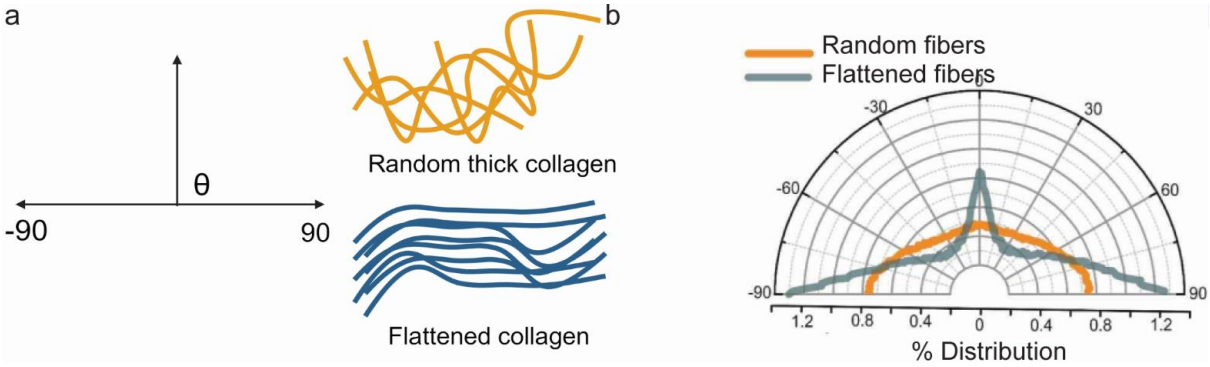

Figure 4. Orientation Analysis Collagen Fiber; a. Random and flattened fiber orientation, b. Output from OrientationJ in Image J of Random and Flattened Fibers.

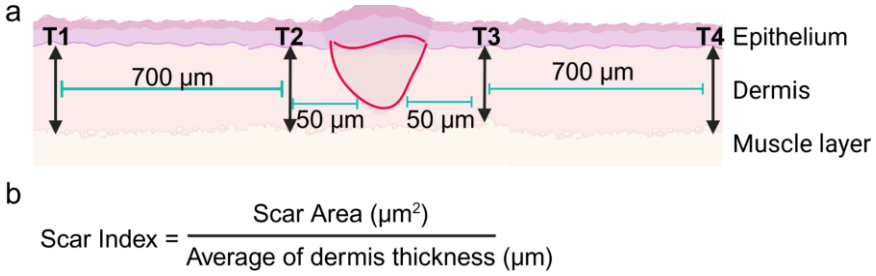

Figure 5. The measurement of scar volume under a light microscope using HE staining. a. A picture showing the Scar Index parameter in HE staining of skin. b. The Scar Index computation formula. Reproduced from Khorasani et al. (2011). Modified from Khorasani and colleagues (2011).

Clemons, *et al*, (2018) employed coherence image analysis to address subjectivity in assessing collagen fibers within fibroblast cultures. They quantitatively measured the degree of fiber orientation. Collagen was stained with immunocytochemicals at the cellular level and examined with fluorescence microscopy. The OrientationJ plugin in ImageJ was employed to conduct additional analysis on the generated fluorescence images (developed by Clemons *et al*., 2018). According to Rezakhaniha *et al*. (2012), OrientationJ applies the structural tensor approach per pixel in the spatial domain. The alignment and sampling of thick, flat collagen fibers at random, represent both normal, healthy skin and skin with scars (Figure 4a). In healthy skin, collagen orientation is evenly distributed between -90° and 90°. However, in scarred skin, the prominent orientations are -90° and 90°. This image-based qualitative analysis can also be extended to other biological fibers, including F-actin, microtubules, and vascular networks. Further advancements in fiber analysis, particularly the TWOMBLI plugin published by Wershof *et al*. (2021) enhance our understanding of tissue damage matrix features using ImageJ.

Quantitative Analysis of Collagen Fiber
Scar Index Quantification

The collagen density, thickness, and orientation of scars differ from those of the intact dermis in several ways. As the main extracellular matrix (ECM) protein in both healthy and damaged skin, collagen has led to the development of many assays to look at different aspects of its structure (Clemons *et al*., 2018). A previous investigation established the scar index by dividing the scar surface area by the usual skin thickness around the scar. Skin thickness, a sign of tissue regeneration, is measured 50–700 µm away from the scar area, (Figures 5a–5b) (Khorasani *et al*., 2011). Instead of using HE stains, Masson's trichrome staining method is employed to calculate the scar index.

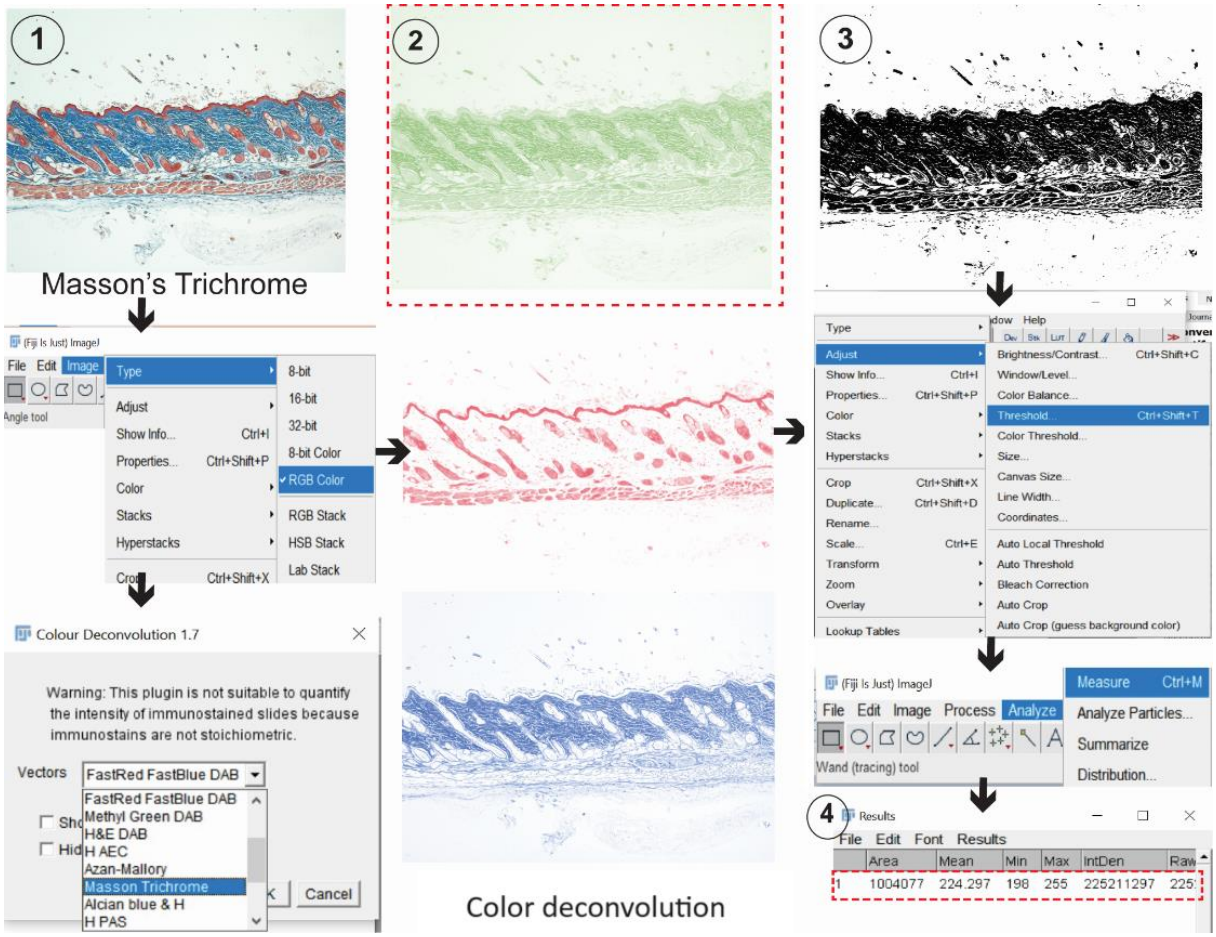

Figure 6. Collagen fiber quantification with ImageJ's Color Deconvolution method. Step 1: Masson's staining and file type selection Step 2: The image was divided into sections that were blue, red, and green. Step 3: Modifying the upper limit Step 4: Utilizing the integrated density measurement to analyze the image. Adapted from Chen *et al.* (2017).

This method imparts a blue-green color to collagen fibers when viewed under a light microscope (Kanitakis, 2013). Its versatility extends to various wound healing studies, pharmaceutical evaluations, biomedical devices, and surgical procedures (Djatumurti *et al.*, 2021; Setiawati *et al.*, 2021).

Collagen Content Measurement Using ImageJ

In addition to HE staining, researchers have employed alternative staining methods such as Masson's Trichrome and Picrosirius Red to assess collagen content in tissue sections (Whittaker *et al.*, 1994; Chen *et al.*, 2017; Benito-Martínez *et al.*, 2022). Collagen content serves as an indicator not only for skin healing but also for aging processes and other pathophysiological changes in atherosclerotic lesions (Osman *et al.*, 2014; Wersof *et al.*, 2021). A previous study evaluated collagen content in wounded skin using the hydroxyproline assay (Pananchery & Gadgoli, 2021).

In many comparative studies, the first step is to use ImageJ, an image-processing program developed by the National Institutes of Health (NIH) and the Laboratory for Optical and Computational Instrumentation (LOCI) at the University of Wisconsin (https://imagej.net/). According to Schneider *et al.* (2012), Image J is an open-source, 64-bit Java application designed specifically as a plugin.

Assessing collagen content in skin tissue using Masson's trichrome staining begins with staining the skin tissue. The stained skin tissue images were captured at a minimum resolution of

640 x 280 pixels in 24-bit RGB and saved in Tagged Image File Format (TIFF). To perform collagen quantification, researchers follow these four steps. The Masson trichrome-stained image of the skin is first prepared by opening it in ImageJ software and determining whether it should be in RGB format for analysis (Figure 6). The Color Deconvolutions Plugin is then used to process the RGB image further in order to extract collagen bundles from additional overlapping regions. During the development of the color image, Masson's tricolor patch was developed into red, blue, and green layers. In step 2 of Figure 6, the green layer was detected as collagen fibers. Now focus on the green layer, this should be thresholded to the identical level for every sample compared in step 3. Last, we analyzed the collagen content in the sample in step 4. In comparative studies, it is crucial to set the scale for every image in ImageJ. During the process of color deconvolution, images are captured using consistent magnification levels and the same instrument. This ensures uniform resolution for each color channel. In our study, we acquired images at a resolution of 2560 x 1920 pixels, optimizing performance. The technique of color deconvolution provides a rapid and convenient approach for quantifying collagen content in applied research. Researchers can express the data on collagen fiber content either as an absolute number or as a percentage of the total collagen present.

OrientationJ can draw vector fields and exhibit directional analysis on fibers, but this does not provide the quantification of whole matrix patterns. Previous studies attempted a complicated manual data analysis intervention to quantify supplementary matrix metrics (Manning *et al*. 2015; Rezakhaniha *et al*. 2012). Another image analysis plug-in in ImageJ used to quantify fibrillar structures is FibrilTool, which is based on the concept of a nematic tensor providing a quantitative description of fiber arrays and orientation in cells. It has already been successfully applied to cortical microtubules in plant cells and cellulose microfibers. Thus, it may help to analyze collagen fiber orientation in each region of interest (ROI) with almost no smoothing needed (Boudaoud *et al*. 2014).

Investigating a broad metrics range relating to one aspect of ECM organization is a challenging and time-consuming method. Therefore, to quantify ECM patterns, an end-to-end pipeline that is automated and easy to use is needed to be applied to versatile data sets. Previous studies had created another macro plugin of imageJ; called TWOMBLI standing for The Workflow of Matrix Biology Informatics. This plugin quantifies matrix patterns based on ECM images by acquiring a range of metrics, which could be connected to the clinical data if needed. TWOMBLI can produce reliable metrics with, same as color deconvolution, must follow common principles of image acquisition and analysis parameters. It could provide a quantitative framework for differentiating between different ECM architectures. The multiple parameters of fiber analysis with the TWOMBLI plugin were not only isotropic and anisotropics, but also lacunarity, fractal dimension, matrix density, and curvature (Rezakhaniha *et al*. 2012).

CONCLUSION

Assessing the dermal layer's collagen fiber content and alignment is essential for monitoring the development of tissue regeneration and wound healing. Collagen deposition in the dermal granulation tissue exceeds the epidermal thickness layer during the skin's healing process (Brianezi *et al*., 2015). Traditionally, collagen fiber density assessment relies on visual evaluation by trained experts, using a subjective 0 to 4+ scoring system. However, this method results in low precision and significant subjectivity (Chipala *et al*., 2020). As a result, in both laboratory and clinical settings, determining quantitative markers for objectively assessing collagen density and organization remains a challenge. Furthermore, the alignment of collagen fibers plays a crucial role in assessing scarring potential. Limandjaja *et al*. (2017) and Zhou *et al*. (2019) reveal that normal collagen fibers exhibit a thick and random orientation, whereas scar tissue displays thin and flattened collagen fibers. Recent studies have explored image-based analyses using popular free software tools like ImageJ. For qualitative assessment, tools like OrientationJ and the recently developed TWOMBLI Plugin prove useful. Meanwhile, the Color Deconvolution Plugin accurately calculates collagen content and density. These insights offer promising avenues for reliable methods to assess wound healing quantitatively and qualitatively. Such approaches can be applied in drug delivery studies aimed at enhancing wound healing outcomes.

ACKNOWLEDGMENTS

There was no funding authority granted a specific financial project for this work.

CONFLICT OF INTEREST

The authors declare no conflict of interest.

REFERENCES

Babalola, O., Mamalis, A., Lev-Tov, H., & Jagdeo, J. (2014). Optical coherence tomography (OCT) of collagen in normal skin and skin fibrosis. *Arch. Dermatol. Res.* , 306(1), *1–9*. https://doi.org/10.1007/s00403-013-1417-7

Benito-Martínez, S., Pérez-Köhler, B., Rodríguez, M., Izco, J. M., Recalde, J.I., & Pascual, G. (2022). Wound healing modulation through the local application of powder collagen-derived treatments in an excisional cutaneous murine model. *Biomedicines,* 10(5), 960. https://doi.org/10.3390/biomedicines10050960.

Boniakowski, A. E., Kimball, A. S., Jacobs, B. N. , Kunkel, S. L., & Gallagher, K. A. (2017). Macrophage-mediated inflammation in normal and diabetic wound healing. *J. Immun. J.,* 199(1), *17–24*. https://doi.org/10.4049/jimmunol.1700223.

Boudaoud, A.E., Burian A., Borowska-Wyzkret, D., Uyttewaal, M., Wrzalik , R., Kwiatkowska D., Haman*t,* O. (2014). FibrilTool, an ImageJ plug-in to quantify fibrillar structures in raw microscopy images. *Nat Protoc.* 9(2): 457-63.https://doi.org/10.1038/nprot.2014.024.

Brauer, E., Lippens, E., Klein, O., Nebrich, G., Schreivogel, S., Korus, G., Duda, G. N., & Petersen, A. (2019). Collagen fibrils mechanically contribute to tissue contraction in an in vitro wound healing scenario. *Adv. Sci*, 6(9), 1801780. https://doi.org/10.1002/advs.201801780.

Brianezi, G., Grandi, F., Bagatin, E., Enokihara, M. M. S. S., & Miot, H. A. (2015). Dermal type I collagen assessment by digital image analysis. *An. Bras. Dermatol.,* 90(5), 723–727. https://doi.org/10.1590/abd1806-4841.20153331.

Brianezi, L. , Ornelas, E. , Gehrke F.S. , Fonseca F.L.A. , Alves B.D.C.A. , Sousa L.V.A. , Souza J., Maifrino L.B.M. (2020) . Effects of Physical Training on the Myocardium of Oxariectomized LDLr Knockout Mice: MMP 2/9, Collagen I/III, Inflammation and Oxidative Stress. *Arq Bras Cardiol*. 1141:100-105.https://doi.org/10.5935/abc.20190223.

Bien, P., De Anda C., Prokocimer, P. (2014). Comparison of digital planimetry and ruler technique to measure absssi lesion sizes in the ESTABLISH-1 Study. *Surgical Infection*. 15, 2. https://doi.org/10.1089/sur.2013.070

Brook, I. (1995). Microbiology of gastrostomy site wound infections in children. *J. Med. Microbiol.*, 43(3), 221–223. https://doi.org/10.1099/00222615-43-3-221.

Caetano, G. F., Fronza, M., Leite, M. N., Gomes, A., & Frade, M. A. C. (2016). Comparison of collagen content in skin wounds evaluated by biochemical assay and by computer-aided histomorphometric analysis. , *Pharm. Biol*. 54 (11), 2555–2559.https://doi.org/0.3109/13880209.2016.1170861

Caley, M.P., Martins, V. L. C., & O'Toole, E.A. (2015). Metalloproteinases and wound healing. *Adv Wound Care,* 4(4), 225–234. https://doi.org/10.1089/wound.2014.0581

Chen, W.T. (1992). Membrane proteases: Roles in tissue remodeling and tumor invasion. *Curr. Opin. Cell Biol.,* 4(5), 802–809. https://doi.org/10.1016/0955-0674(92)90103-j

Chen, Y., Yu, Q., & Xu, C. B. (2017). A convenient method for quantifying collagen fibers in atherosclerotic lesions by image j software. *Int J Clin Exp Med* 10(10), 14904–14910.

Chlipala, E., Bendzinski, C. M., Chu, K., Johnson, J. I., Brous, M., Copeland, K., & Bolon, B. (2020). Optical density-based image analysis method for the evaluation of hematoxylin and eosin staining precision. *J. Histotechnol.*, 43(1), 29–37. https://doi.org/10.1080/01478885.2019.1708611.

Clark, R. A. F. (2003). Fibrin is a many splendored thing. *J Invest Dermatol,* 121(5), 21-22. https://doi.org/10.1046/j.1523-1747.2003.12575.x.

Clemons, T. D., Bradshaw, M., Toshniwal, P., Chaudari, N., Stevenson, A., Lynch, J., Fear, M. W., Wood, F. M., & Iyer, K. S. (2018). Coherency image analysis to quantify collagen architecture: implications in scar assessment. *RSC Advances,* 8(18), 9661-9669. https://doi.org/10.1039/C7RA12693J

Cognasse, F., Hamzeh, H., Chavarin, P., Acquart, S., Genin, C., & Garraud, O. (2005). Evidence of

toll-like receptor molecules on human platelets. *Immunol. Cell Biol.,* 83(2), 196–198. https://doi.org/10.1111/j.1440-1711.2005.01314.x

Desmouliere, A., Redard, M., Darby, I., & Gabbiani, G. (1995). Apoptosis mediates the decrease in cellularity during the transition between granulation tissue and scar. *Am J Pathol* 146(1), 56–66

Dhane, D. M., Maiti, M., Mungle, T., Bar, C., Achar, A., Kolekar, M., & Chakraborty, C., (2017). Fuzzy spectral clustering for automated delineation of chronic wound region using digital images. *Comput. Biol. Med.*, 2017; 89, 551-560. http://dx.doi.org/10.1016/j.compbiomed.2017.04.004.

Dhane, D. M., Khrisna, V., Achar A., Bar, C., Sanyal, K., & Chakraborty, C. (2016). Spectral clustering for unsupervised segmentation of lower extremity wound beds using optical images. *J Med Syst*, 40(9), 207. https://doi.org/10.1007/s10916-016-0554-x.

Dhasmana, A., Singh, L., & Malik S. (2021). Smart Bio-Polymeric Matrix for Accelerated Wound Healing and Tissue Regeneration. *Austin J Biomed Eng*. 6(1):1045. https://doi.org/10.26420/austinjbiomedeng.2021.1045.

Djatumurti, D. R., Rafida, A., & Manalu, A. Y. P., & Pangestiningsih, T. W. (2021). Re-epithelization and density of collagen fibers on wound healing of mice's skin (*Mus musculus*) that treated with combination of chitosan membrane and eel (*Monopterus albus*) mucous. *BIO Web of Conferences*, 33, 06005. https://doi.org/10.1051/bioconf/20213306005

Dong R. & Guo B. (2021). Smart wound dressings for wound healing. Nanotoday. 41:101290. https://doi.org/10.1016/j.nantod.2021.101290.

Duong, T. E., & Hagood, J. S. (2018). Epigenetic regulation of myofibroblast phenotypes in fibrosis. *Curr. Pathobiol. Rep*, 6(1), 79–96. https://doi.org/10.1007/s40139-018-0155-0.

Enoch, S., & Leaper, D. J. (2008). Basic science of wound healing. *Surgery,* 23(2), 37–42. https://doi.org/10.1383/surg.23.2.37.60352.

Freedman, B.R., Hwang C., Talbot S., Hibler, B. & Mooney, D.J., (2023). Breakthrough treatments for accelerated wound healing. *Sci. Adv.*, 9(20). eade700. https://doi.org/10.1126/sciadv.ade7007.

Filko, D., & Nyarko, E. K. (2023). 2D/3D wound segmentation and measurement based on a robot-driven reconstruction system. *Sensors*, 23(6), 1-23. https://doi.org/10.3390/s23063298

Folkman, J., & D'Amore, P. A. (1996). Blood vessel formation: What is its molecular basis? *Cell*, 87(7), 1153–1155. https://doi.org/10.1016/s0092-8674(00)81810-3

Foltynski, P., Ladyzynski P., Ciechanowska, A., Migalska-Musial, K., Judzewicz, G., & Sabalinska, S. (2015). Wound area measurement with digital planimetry: improved accuracy and precision with calibration based on 2 rulers. *PLoS ONE*, 10(8), 1-13. https://doi.org/10.1371/journal.pone.0134622

Gnyawali, S., C., Sinha, M., El Masry, M., S., Wulff, B., Ghatak, S., Soto-Gonzalez, F., Wilgus, T., A., Roy, S., & Sen, C., K. (2020). High resolution ultrasound imaging for repeated measure of wound tissue morphometry, biomechanics and hemodynamics under fetal, adult and diabetic conditions. *PLoS ONE*, 15(11), 1-23. https://doi.org/10.1371/journal.pone.0241831.

Gole, L., Yeong, J., Lim, J. C. T., Ong, K. H., Han, H., Thike, A. A., Poh, Y. C., Yee, S., Iqbal, J., Hong, W., Lee, B., Yu, W., & Tan, P. H. (2020). Quantitative stain-free imaging and digital profiling of collagen structure reveal diverse survival of triple negative breast cancer patients. *Breast Cancer Res*, 22:42. https://doi.org/10.1186/s13058-020-01282-x

Golebiewska, E. M., & Poole, A.W. (2015). Platelet secretion: From haemostasis to wound healing and beyond. *Blood Rev.,* 29(3), 153–162. https://doi.org/10.1016/j.blre.2014.10.003

Guo, S., & DiPietro, L. A. (2010). Critical review in oral biology & medicine: Factors affecting wound healing. *J. Dent. Res.,* 89(3), 219–229. https://doi.org/10.1177/0022034509359125.

Gurtner, G. C., Werner, S., Barrandon,Y., & Longaker, M. T. (2008). Wound repair and

regeneration. *Nature*, 453(7193), 314–321. https://doi.org/10.1038/nature07039.

Gynawali, S.C., Sinha, M., El Masry M.S., Wulf, B., Ghatak, S., Gonzales, F.S., Wilgus, T.A., Roy, S., Sen, C.K. (2020). High-resolution harmonics ultrasound imaging for non-invasive characterization of wound healing in a pre-clinical swine model. *PLoS One*. 5(11):e0241831. https://doi.org/10.1371/journal.pone.0241831.

Ho, J.K. & Hantash, B.M. (2013). The principles of wound healing. *Expert Rev. Dermatol*. 8(6), 639–658. https://doi.org/10.1586/17469872.2013.857161.

Huang, C., Wu, Z., Du, Y., & Ogawa, R. (2020). The epidemiology of keloids. In *Textbook on Scar Management* (pp. 20). Springer, Cham

Huang, S.P., Wu, M., Shun, C., Wang, H., Hsieh, C., Kuo, M, & Lin, J. (2005). Cyclooxygenase-2 increases hypoxia-inducible factor-1 and vascular endothelial growth factor to promote angiogenesis in gastric carcinoma. *J. Biomed. Sci.,* 12(1), 229–241. https://doi.org/10.1007/s11373-004-8177-5.

Jin, J., Li, H., Chen, Z., Sheng, J., Liu, T., Ma, B., Zhu, S., & Xia, Z. (2018). 3-D wound scanner: a novel, effective, reliable, and convenient tool for measuring scar area. *Burns.* 44(8), 1930-1939. https://doi.org/10.1016/j.burns.2018.05.009.

Jørgensen, L. B., Halekoh, U., Jemec G. B. E., Sørensen, J. A., & Yderstræde, K. B. (2020). monitoring wound healing of diabetic foot ulcers using two-dimensional and three-dimensional wound measurement techniques: a prospective cohort study. *Adv Wound Care (New Rochelle)*, 9(10), 554–555. https://doi.org/10.1089/wound.2019.1000

Kanitakis, J. (2002). Anatomy, histology, and immunohistochemistry of normal human skin. *Eur J Dermatol*, 12(4), 390–401.

Kanitakis, J. (2013). Keloidal dermatofibroma: report of a rare dermatofibroma variant in a young white woman. *Am J Dermatopathol,* 35(3), 400-401. https://doi.org/10.1097/DAD.0b013e31825d9d30.

Khorasani, H., Zheng, Z., Nguyen, C., Zara, J., Zhang, X., Wang, J., Ting, K. & Soo, C. (2011). A quantitative approach to scar analysis. *Am J Pathol,* 178(2), 621–628. https://doi.org/10.1016/j.ajpath.2010.10.019

Kolimi, P., Narala, S., Nyavanandi D., Youssef A.A.A., & Dudhipala, N., (2022). Innovative treatment strategies to accelerate wound healing: Trajectory and recent advancements. *Cells*. 11(15). 2439. https://doi.org/10.3390/cells11152439.

Limandjaja, G. C., Van den Broek, L. J., Waaijman, T., Van Veen, H. A., Everts, V., Monstrey, S., Scheper, R. J., Niessen, F. B., & Gibbs, S., (2017). Increased epidermal thickness and abnormal epidermal differentiation in keloid scars. *Br. J. Dermatol.*176(1), 116–126. https://doi.org/10.1111/bjd.14844

Mahbod, A., Ecker, R., Schaefer, G., & Ellinger, I. (2021). Automatic foot ulcer segmentation using an ensemble of convolutional neural networks. https://doi.org/10.48550/arXiv.2109.01408.

Mathew-Steiner, S. S., Roy, S., & Sen, C. K. (2021). Collagen in wound healing. *Bioengineering,* 8(5), 63. https://doi.org/10.3390/bioengineering8050063.

Matsumoto, M., Nakagami, G., Kitamura, A., Kurita M., Suga, H., Miyake, T., Kawamoto, A., & Sanada, H. (2021). Ultrasound assessment of deep tissue on the wound bed and peri-wound skin: a classification system using ultrasound images. *J. Tissue Viability* 30(1), 28-35. https://doi.org/10.1016/j.jtv.2020.08.002

McGibbon, D. (2005). Rook's Textbook of Dermatology, 7th edition *Clin Exp Dermatol* 31(1), 178–179. https://doi.org/10.1111/j.1365-2230.2005.02034.x

McGrath, J. A. (2020). The structure and function of the skin. In *McKee's Pathology of The Skin With Clinical Correlations*, 5th edition, volume 1 (pp. 26). Elsevier, Edinburgh

Mirhaj, M, Labbaf S., Tavakoli M., & Seilafan, A.M., Emerging treatment Strategies in Wound care. (2022). *nt. Wound J*. 13786. https://doi.org/10.1111/iwj.13786.

Moulin, V., Larochelle, S., Langlois, C., Thibault, I., Lopez-Vallé, C. A., & Roy, M. (2004). Normal skin wound and hypertrophic scar myofibroblasts have differential responses to apoptotic inductors. *J. Cell. Physiol.,*

198(3), 350–358. https://doi.org/10.1002/jcp.10415.

Murphy, P. S., & Evans, G. R. D. (2012). Advances in wound healing: a review of current wound healing products. *Plast. Surg. Int.* 190436. https://doi.org/10.1155/2012/190436

Naik, S., Bouladoux, N., Linehan, J. L., Han, S., Harrison, O. J., Wilhelm, C., Conlan, S., Himmelfarb, S., Byrd, A. L., Deming, C., Quinones, M., Brenchley, J. M., Kong, H. H., Tussiwand, R., Murphy, K. M., Merad. M., Segre, J. A., & Belkaid, Y. (2015). Commensal-dendritic-cell interaction specifies a unique protective skin immune signature. *Nature*, 520(7545), 104-108. https://doi.org/10.1038/nature14052

Mutiah, R., Firsyaradha, W. Y., Sari, R. A., Annisa, R., Kristanti, R. A., Indrawijaya, Y. Y. A., Griana, T. P., & Listiyana, A. (2020). Eleutherine Palmifolia (l.) merr. The extract increases the crypts and caspase-3 expression in colitis-associated colon cancer model. *Indonesian J. Pharm.*31(4), 257-265. https://doi.org/10.22146/ijp.1120.

Nurrahma, H.A., Meliala, A., Narwidina, P., Herwiyanti, S. (2021) Hepatoprotective Effect of Banana Peel Flour on Histological and Liver Function in Diabetic Rats. Indonesian J Pharm. 32(4): 529-638, https://doi.org/10.22146/ijp.1917.

Osman, O. S., Selway, J. L., Harikumar, P.E., Jassim, S., & Langlands, K. (2014). Automated analysis of collagen histology in ageing skin. *Proceedings of The International Conference on Bioimaging* (*Bioimaging 2014),* 41-48, https://doi.org/10.5220/0004786600410048

Owczarzy, A., Kurasiński, R., Kulig, K., Rogóż, W., Szkudlarek, A., & Maciążek-Jurczyk, M. (2020). Collagen-structure properties and application. *Eng. Biomat,* 156. 17-23. https://doi.org/10.34821/eng.biomat.156.2020.17-23

Pananchery, J., & Gadgoli, C. (2021). In-vivo evaluation of phytosomal gel of the petroleum ether extract of root bark of onosma echiodes for wound healing activity in rats. *Indonesian J. Pharm,* 32(4), 474-483. https://doi.org/10.22146/ijp.2351

Petrov V.V., Fagard R.H., Lijnen, P.J. (2002), Stimulation of Collagen Production by Transforming Growth Factor-β1 During Differentiation of Cardiac Fibroblasts to Myofibroblasts. *Hyperthension* 39:258–263. https://doi.org/10.1161/hy0202.103268.

Pfisterer, K., Shaw, L. E., Symmank, D., & Weninger, W. (2021). The extracellular matrix in skin inflammation and infection. *Front. Cell Dev. Biol.* 9, 682414. https://doi.org/10.3389/fcell.2021.682414.

Potekaev, N. N., Borzkyh, O. B., Medvedev, G. V., Pushkin, D. V., Petrova, M. M., Gavrilyuk, O. A., Karpova, E. I., Trefilova, V. V., Deminas, O. M., Popova, T. E. & Shanayder, N. A. (2021). Genetic and epigenetic aspects of skin collagen fiber turnover and functioning. *Cosmetics*, 8(4), 92. https://doi.org/10.3390/cosmetics8040092.

Quan, T., & Fisher, G. J. (2015). Role of age-associated alterations of the dermal extracellular matrix microenvironment in human skin aging: a mini-review. *Gerontology.* 2015;61(5), 427–434. https://doi.org/10.1159/000371708

Rangaraj, A., Harding, K., & Leaper, D. (2011). Role of collagen in wound management. *Wounds UK,* 7(2), 54–63

Rezakhaniha, R., Agianniotis, A., Schrauwen, J. T. C., Griffa, A., Sage, D., Bouten, C. V. C., Van de Vosse, F. N., Unser, M., & Stergiopulos, N. (2012). Experimental investigation of collagen waviness and orientation in the arterial adventitia using confocal laser scanning microscopy. *Biomech. Model. Mechanobiol.,* 11(3-4):461–473. https://doi.org/10.1007/s10237-011-0325-z

Rodrigues, M., Kosaric, N., Bonham, C. A., & Gurtner, G.C. (2019). Wound healing: A cellular perspective. *Physiol. Rev.,* 99(1), 665–706. https://doi.org/10.1152/physrev.00067.2017

Sabol, F., Dancakova, L, Gál, P. Vasilenko, T., Novotny, M., Smetana, K., & Lenhards, L. (2012). Immunohistological changes in skin wounds during the early periods of healing in a rat model. *Vet. med.,* 57, 77–82. https://doi.org/10.17221/5253-VETMED.

Scebba, G., Zhang, J., Catanzaro, S., Mihai, C.,Distler, O., Berli, M., & Walter, K. (2022). Detect-and-segment: A deep learning approach to automate wound image segmentation. *Inform. Med. Unlocked*, 29:100884. https://doi.org/10.1016/j.imu.2022.100884.

Schipke, J., Brandenbergeer, C., Rajces, A., Manninger, M., Alogna, A., Post, H., & Mühlfeld, V. (2017). Assessment of cardiac fibrosis: a morphometric method comparison for collagen quantification. *J. Appl. Physiol.*, 122: 1019-1030. https://doi.org/10.1152/japplphysiol.00987.2016

Schneider, C. A., Rasband, W. S., & Eliceiri, K. W., (2012). NIH Image to ImageJ: 25 years of image analysis. *Nat. Methods.* 9 (7): 671–675. https://doi.org/10.1038/nmeth.2089.

Senejko, M., Pasek, J., Szajkowski, S., Cieślar, G., & Sieroń, A. (2021). Evaluation of the therapeutic efficacy of active specialistic medical dressings in the treatment of decubitus. *Postepy Dermatol Alergol.* 38(1), 75-79. https://doi.org/10.5114/ada.2021.104282.

Setiawati, A., Jang, D., Cho, D., Cho, S., Jeong, H., Park, S., Gwak, J., Ryu, S. R., Jung, W. H., Ju, B., Jung, K., Kwon, O., & Shin, K. (2021). An accelerated wound-healing surgical suture engineered with an extracellular matrix. *Adv. Healthc. Mater.,* 10(6), 1–10. https://doi.org/10.1002/adhm.202001686.

Singer, A. J., & Clark, R. A. (1999). Cutaneous wound healing. *The new england journal of medicine*, 341(10), 738-746. https://doi.org/10.1056/NEJM199909023411006.

Somaiah, C., Kumar, A., Mawrie, D., Sharma, A., Patil, S. D., Bhattacharyya, J., Swaminathan, R., & Jaganathan, B. G. (2015). Collagen promotes higher adhesion, survival, and proliferation of mesenchymal stem cells. *PLoS One,* 10(120), 1–15. https://doi.org/10.1371/journal.pone.0145068.

Takeo, M., Lee, W., & Ito, M. (2015). Wound healing and skin regeneration. Cold spring harbor *Perspective in Medicine*, ;5:a023267. https://doi.org/10.1101/cshperspect.a023267

Tang, Y. Q., Yeaman, M. R., & Selsted, M.E. (2002). Antimicrobial peptides from human platelets. *Infect. Immun.,* 70(12), 6524–6533. https://doi.org/10.1128/IAI.70.12.6524-6533.2002

Theunissen D., Seymour B., Forder M, Cox S.G., Rode H. (2016). Measurements in wound healing with observations on the effects of topical agents on full thickness dermal incised wounds. *Burns.* 42(3):556-63.

Theocharis, A. D., Skandalis, S. S., Gialeli, C., & Karamanos, N. K. (2016). Extracellular matrix structure. *Adv. Drug Deliv. Rev.* 1(97), 4–27. https://doi.org/10.1016/j.addr.2015.11.001.

Velez, A. M. A, & Howard, M. S. (2012). Collagen IV in normal and in disease process. *N. Am. J. Med. Sci.,* 4(1), 1–8. https://doi.org/10.4103/1947-2714.92892.

Velnar, T., Bailey, T., & Smrkolj, V. (2009). The wound healing process: An overview of the cellular and molecular mechanisms. *Int. J. Med. Res.*, 37(5), 1528–1542. https://doi.org/10.1177/147323000903700531.

Verhaegen, P. D. H. M, Van Zujilen, P. P. M., Pennings, N. M., Van Marle, J., Niessen, F. B., Van der Horst, C. M. A. M., & Middelkoop, E. (2009). Differences in collagen architecture between keloid, hypertrophic scar, normotrophic scar, and normal skin: an objective histopathological analysis. *Wound Repair Regen.* 17(5), 649–656. https://doi.org/10.1111/j.1524-475X.2009.00533.x

Wang, H. (2021). A review of the effects of collagen treatment in clinical studies. *Polymers*, 13(22), 3868. https://doi.org/10.3390/polym13223868.

Wang, C., Anisuzzaman, D., M., Williamson, V., Dhar, M., K., Rostami, B., Niezgoda, J., Gopalakrishnan, S., & Zeyun, Y. (2020). Fully automatic wound segmentation with deep convolutional neural networks. *Scic Rep.,* 10(1), 1-9. https://doi.org/10.1038/s41598-020-78799-w

Wardani, I G. A. A. K., Jawi, I M., Senapathi, T. G. A., Sanjaya, D. A., Antari, N. P. U., Adrianta, K. A., & Suena, N. M. D. S. (2022). The effect of Xylocarpus granatum j. koenig seed extract cream on the number of fibroblast and re-epithelialization in IIA degree burn wound healing. *Indonesian J. Pharm.*, 33(4), 653-665. https://doi.org/10.22146/ijp.3461

Wershof, E., Park, D., Barry, D. J., Jenkins, R. P., Rulan, A., Wilkins, A., Schlegelmilch, K, Roxanis, I, Anderson, K. I., Bates, P. A., & Sahai, E. (2021). A FIJI macro for quantifying patterns in extracellular matrix. *Life Sci. Alliance,* 4(3), 1–11. https://doi.org/10.26508/lsa.202000880

Whittaker, P., Kloner, R. A., Boughner, D. R., & Pickering, J. G. (1994). Quantitative assessment of myocardial collagen with picrosirius red staining and circularly polarized light. *Basic Res Cardiol*. 89(5), 397–410. https://doi.org/10.1007/BF00788278.

Wilkinson, H. N., & Hardman, M. J. (2020). Wound healing: cellular mechanisms and pathological outcomes. *Open Biol.,* 10. 200223. https://doi.org/10.1098/rsob.200223

Wolfram, D., Tzankov, A., Pülzl, P., & Piza-Katzer, H. (2009). Hypertrophic scars and keloids - a review of their pathophysiology, risk factors, and therapeutic management. *Dermatol. Surg.*, 35(2), 171-181. https://doi.org/171–181.10.1111/j.1524-4725.2008.34406.x.

Xue, M., & Jackson, C. J. (2015). Extracellular matrix reorganization during wound healing and its impact on abnormal scarring. *Adv Wound Care,* 4(3), 119–136. https://doi.org/10.1089/wound.2013.0485

Yang, H. J., & Kang, S.Y. (2019). The clinical uses of collagen-based matrices in the treatment of chronic wounds. *J Wound Manag Res.*, 15(2), 103-108. https://doi.org/10.22467/jwmr.2019.00640.

Zaidi, A., & Green, L. (2019). Physiology of haemostasis. *Anaesth Intensive Care*, 20(3), 152–158. https://doi.org/10.1016/j.mpaic.2019.01.005

Zhou, S., Wang, W., Zhou, S., Zhang, G., He, J., & Li, Q. (2019). A novel model for cutaneous wound healing and scarring in the rat. *Plast. Reconst. Surg.,* 2019;143(2):468–477. https://doi.org/10.1097/PRS.0000000000005274

Zhu, Z., Ding, J., Shankowsky, H. A., & Tredget, E.E. (2013). The molecular mechanism of hypertrophic scar. *Cell Commun Signal.*, 7(4), 239–252. https://doi.org/10.1007/s12079-013-0195-5.